

Quasiconformal Mappings for Surface Mesh Optimization

ANTHONY GRUBER, Florida State University
EUGENIO AULISA, Texas Tech University

Quasiconformal mappings from surfaces immersed in Euclidean space are discussed for the purposes of computing dilatation-optimal surface meshes with prescribed connectivity and Dirichlet boundary data. In particular, it is shown that optimal quasiconformal mappings can be characterized as constrained critical points of the usual Dirichlet energy with respect to a certain Riemannian metric, leading to an iterative algorithm for the computation of discrete mesh transformations which minimize the maximal conformality distortion of each element. Based on the established Quasiconformal Iteration method, the proposed algorithm produces high quality surface mappings which correctly capture boundary information while eliminating undesirable folds which can appear during least-squares conformal mapping procedures.

CCS Concepts: • Computing methodologies → Shape modeling; • Mathematics of computing → Partial differential equations.

Additional Key Words and Phrases: quasiconformal mapping, Teichmüller mapping, mesh optimization, surface remeshing

ACM Reference Format:

Anthony Gruber and Eugenio Aulisa. 2021. Quasiconformal Mappings for Surface Mesh Optimization. *ACM Trans. Graph.* 37, 4, Article 111 (June 2021), 14 pages. <https://doi.org/10.1145/nmnnnn.nmnnnn>

1 INTRODUCTION

Conformal maps between two-dimensional Riemann surfaces are widely recognized as useful tools in both theoretical and computational settings. In particular, enough interesting quantities are conformally invariant (e.g. the total Gaussian curvature and the Willmore energy of surfaces) that many difficult problems can be made considerably simpler by applying an appropriate conformal transformation. Moreover, at the present time there are several effective algorithms for computing conformal or nearly conformal mappings (see e.g. [Bobenko et al. 2015; Gu et al. 2004; Kharevych et al. 2006; Sawhney and Crane 2017; Springborn et al. 2008; Trefethen 2020] and references therein), the use cases of which cover everything from surface flattening to medical image registration.

Despite their numerous advantages, it is also well known that conformal maps are woefully unsuited to mapping problems with a pointwise boundary correspondence. In particular, there is very often no conformal map between two connected surfaces which maps boundaries to boundaries in a prescribed way, even in quite

Authors' addresses: Anthony Gruber, anthony.gruber@ttu.edu, Florida State University, 600 W College Ave, Tallahassee, Florida, 32306; Eugenio Aulisa, eugenio.aulisa@ttu.edu, Texas Tech University, P.O. Box 41042, Lubbock, Texas, 79409.

Permission to make digital or hard copies of all or part of this work for personal or classroom use is granted without fee provided that copies are not made or distributed for profit or commercial advantage and that copies bear this notice and the full citation on the first page. Copyrights for components of this work owned by others than ACM must be honored. Abstracting with credit is permitted. To copy otherwise, or republish, to post on servers or to redistribute to lists, requires prior specific permission and/or a fee. Request permissions from permissions@acm.org.

© 2021 Association for Computing Machinery.
0730-0301/2021/6-ART111 \$15.00
<https://doi.org/10.1145/nmnnnn.nmnnnn>

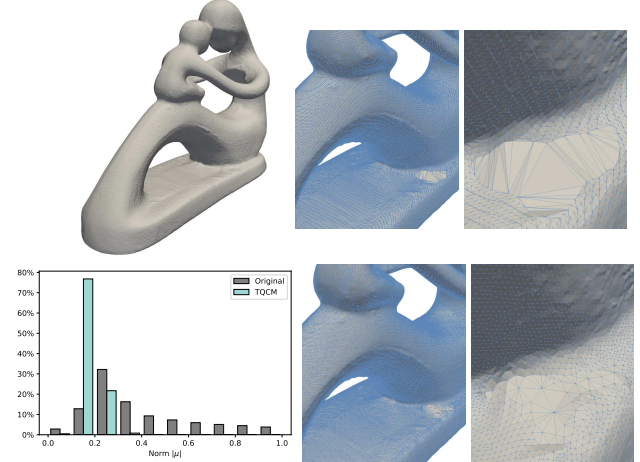


Fig. 1. Teichmüller quasiconformal remeshing (TQCM) of a statue mesh with genus four. Top: remeshed surface; close-up images of original surface. Bottom: histogram of conformality distortion; close-up images of remeshed surface.

simple cases. For example, it can be shown that there is no corner-preserving conformal mapping from a square onto a rectangle. Indeed, no matter the ratio of lengths, there is an inevitable amount of shearing distortion that occurs which is inherently non-conformal. This presents a significant challenge for computational applications which involve some form of mesh deformation, where a conformal (or close-to-conformal) mapping is desired which satisfies some given boundary data. While least-squares conformal mapping techniques can certainly be applied in this instance, they are known to produce undesirable folds if the target surface is non-convex (see e.g. Figure 2 or Figure 4).

On the other hand, if the condition of conformality is relaxed to that of quasiconformality instead (i.e. uniformly bounded conformality distortion), then such maps are relatively abundant. In fact, a mild growth condition on the distortion at the boundary guarantees the existence and uniqueness of a “best possible” quasiconformal map between two Riemann surfaces (see Theorem 2.3). Known as a Teichmüller mapping, this extremal mapping minimizes the maximal conformality distortion throughout the source domain. As these Teichmüller mappings can in many cases be realized as the unique minimizers of a particular energy functional (c.f. Section 2), they are also relatively computable using conventional numerical minimization techniques, making extremal quasiconformal mapping a valid strategy in situations when an explicit boundary correspondence must be satisfied.

1.1 Related Work

Due to their advantageous properties, quasiconformal (QC) mappings have recently been investigated for a variety of computational applications. This usually involves working with some form of the Beltrami equation $f_{\bar{z}} = \mu f_z$ (see Section 2), which characterizes the QC mapping and can be discretized and solved on a manifold mesh or point cloud. Planar QC mappings are used in [Zeng and Gu 2011] for surface registration by precomposing the computation of the Beltrami coefficient μ with a Ricci flow procedure to homogenize the domain. On the other hand, [Zeng et al. 2012] employ a discrete version of the Yamabe flow to compute planar Teichmüller mappings by evolving a given QC metric to a Teichmüller minimum, while [Nian and Chen 2016] compute similar mappings for isogeometric analysis using B-spline techniques. In a different direction, [Lipman 2012] formulates convex spaces of bounded distortion mappings which are computable and contain QC mappings as a subclass, while [Weber et al. 2012] make use of holomorphic quadratic differentials to formulate a minimization-based method for computing extremal Teichmüller maps between planar domains with boundary, or genus 0 surfaces with additional conformal mapping. Yet another approach is taken in [Lui et al. 2014] where an alternating minimization called “QC Iteration” for computing Teichmüller mappings of planar domains and genus 0 surfaces is developed. This QC iteration is connected to the theory of harmonic mappings in [Lui et al. 2015] and shown to converge under some assumptions.

The available techniques for computing QC maps have since been expanded to include other topological types as well as other forms of data. The work [Meng et al. 2016] develops an algorithm called TEMPO for computing Teichmüller mappings on point clouds. Moreover, QC maps of multiply-connected planar domains with prescribed distortion are computed in [Ho and Lui 2016], and [Lee et al. 2016] compute QC maps between 3D volumes for the purpose of surface registration. The variety of algorithms available for computing QC maps has also led to a number of interesting applications, such as a QC kernel for nearest neighbor calculations in machine learning algorithms [Peng et al. 2004] as well as a method for feature-preserving image resizing [Xu et al. 2018]. In addition, QC mappings have also been used to create origami-like surfaces with prescribed folds [Qiu et al. 2019], and to compute QC rectilinear mappings for planar subdivision surfaces [Yang and Zeng 2020].

1.2 Contributions

Despite the far-reaching interest into quasiconformal mappings, at present there are no methods which are adequate for computing QC mappings between surfaces of nonzero genus. Although the mentioned methods can conceivably be applied piece-wise after cutting each surface along the generators of its fundamental group, it is a nontrivial matter in practice to compose such a procedure with the QC mapping algorithms above. Additionally, there appear to be no algorithms in place for computing QC mappings directly from a non-planar surface of any genus. Instead, non-planar domains must first be mapped conformally to the plane, which is similarly nontrivial and requires additional computational resources.

The present work addresses these issues in the case that the target surface is embedded (or more generally, immersed) in \mathbb{R}^3 by

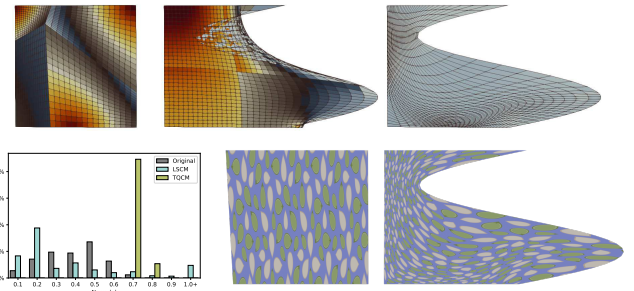


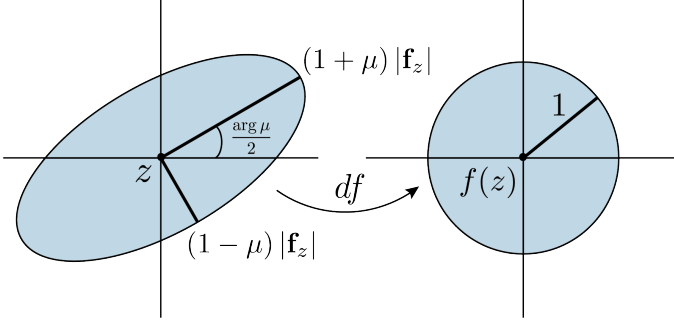
Fig. 2. Comparison between least-squares conformal mapping (LSCM) and Teichmüller quasiconformal mapping (TQCM) on a planar domain with boundary. Note that the LSCM (top mid.) does not respect injectivity, despite producing less overall distortion. (Heatmap in top row colored by $|\mu|$.)

providing a direct algorithm for computing Teichmüller mappings with prescribed Dirichlet boundary conditions, which can be applied to surfaces of arbitrary genus. The approach is based on the Quasiconformal Iteration algorithm of Lui et al. [Lui et al. 2014] mentioned previously, which computes the extremal Teichmüller map $f : M \rightarrow P$ between two connected planar domains, or (with additional conformal mapping) between two connected Riemann surfaces with boundary. In particular, the present work modifies the QC Iteration, extending its applicability to maps from 2-D surfaces which are represented as arbitrary (planar or non-planar) manifold meshes in \mathbb{R}^3 . In this case, the key to a direct algorithm comes from quaternionic surface theory (see e.g. [Burstall et al. 2004; Kamberov et al. 2002]), where the intrinsic notion of quasiconformality is connected to the extrinsic representation of the surface in such a way that QC iteration can be performed directly without the need for conformal pre-processing. Specifically, the present contributions are:

- A self-contained, genus-agnostic algorithm for computing Teichmüller quasiconformal mappings whose domain is a manifold mesh in \mathbb{R}^3 .
- An intrinsic-to-extrinsic formulation of quasiconformal mappings $f : M \rightarrow f(M) \subset \mathbb{R}^3$ which is convenient for computation.
- Applications to surface remeshing and the construction of locally injective mappings satisfying prescribed Dirichlet boundary conditions.

2 MATHEMATICAL PRELIMINARIES

This Section recalls several notions which will be important for the present algorithm, translating them to the quaternionic setting and deriving auxilliary results as necessary. More information regarding the theory of quasiconformal mappings can be found in [Gardiner and Lakic 2000; Hubbard 2006; Strebel 1984], and a good account of the connection between Teichmüller and harmonic mappings is given in [Daskalopoulos and Wentworth 2007]. For a more detailed description of quaternionic surface theory, see [Burstall et al. 2004; Kamberov et al. 2002].

Fig. 3. The geometry of a quasiconformal mapping $f : M \rightarrow \mathbb{R}^3$.

2.1 Extremal Quasiconformal Mappings

Recall that a quasiconformal map $f : M \rightarrow P$ between Riemann surfaces is an orientation-preserving homeomorphism with bounded conformality distortion. More precisely, let (M, g) be a connected Riemann surface with metric g and (possibly empty) boundary ∂M . Then, we say that f is quasiconformal provided it satisfies the *Beltrami equation*,

$$\bar{\partial}f = \partial f \circ \mu$$

where $\partial, \bar{\partial}$ are the \mathbb{C} -linear resp. \mathbb{C} -antilinear parts of the natural derivative operator $df : TM \rightarrow TP$ and $\mu : TM \rightarrow TM$, $|\mu|_\infty < 1$, is the \mathbb{C} -antilinear *Beltrami differential* of the mapping. In a local conformal coordinate $z : U \rightarrow M$ such that $g = \sigma |dz|^2$ for some positive function $\sigma : U \rightarrow \mathbb{R}_+$, this implies the expression

$$f_{\bar{z}} = \mu f_z,$$

where $f_z := \partial_z f$ (resp. $f_{\bar{z}} := \partial_{\bar{z}} f$) are the partial derivatives of the mapping f and $\mu : U \rightarrow \mathbb{C}$, is the locally defined Beltrami coefficient. Note that f is conformal if and only if $\mu \equiv 0$, and this condition depends only on the conformal class of g . Geometrically, the Beltrami equation implies that quasiconformal maps take small circles on the source space to small ellipses of bounded eccentricity on the target. To see this, denote the Euclidean metric by δ and consider a quasiconformal mapping $f : (M, g) \rightarrow f(M) \subset (\mathbb{R}^3, \delta)$. Then, the Jacobian determinant is expressed locally as

$$\text{Jac}(f) = |f_z|^2 - |f_{\bar{z}}|^2 = |f_z|^2 \left(1 - |\mu|^2\right) =: \sqrt{\lambda_1 \lambda_2},$$

where λ_1, λ_2 are the eigenvalues of the pullback metric $f^*\delta$ relative to the flat metric $|dz|^2$. Moreover, since

$$f^*\delta = \langle df, df \rangle = |f_z|^2 |dz + \mu d\bar{z}|^2,$$

these eigenvalues are given by

$$\lambda_1 = |f_z|^2 (1 + |\mu|)^2, \quad \lambda_2 = |f_z|^2 (1 - |\mu|)^2.$$

These are the respective squared lengths of the major resp. minor axes of the ellipse in $T_z(M)$ which pushes forward under df to the unit circle in $T_{f(z)}f(M)$ (c.f. Figure 3). Their ratio defines the maximal dilatation of f ,

$$K(f) = \frac{1 + |\mu|_\infty}{1 - |\mu|_\infty},$$

which is $1 \leq K < \infty$ for orientation-preserving maps and $-\infty < K < -1$ for orientation-reversing maps. Note that $\text{Jac}(f) > 0$ when

$f_z \neq 0$ and $|\mu| < 1$, reflecting the highly important fact that quasiconformal mappings are locally injective. In the discrete setting, this implies that f cannot have foldovers (i.e. places where the mapping fails to be immersive, see Figures 2, 4, and 6), which is essential in applications such as medical device simulations where surfaces must remain embedded as they deform.

Although there may be many quasiconformal mappings from one Riemann surface to another, there are relatively few which are distinguished as being extremal. Moreover, since quasiconformal maps are fundamentally continuous objects, the property of being extremal depends on a given homotopic class of maps into the target space. Indeed, recall that a quasiconformal map $f : M \rightarrow P$ is said to be extremal provided it minimizes the maximal dilatation K in its homotopic class. More precisely, f is extremal provided

$$K(f) \leq K(h),$$

for any map $h : M \rightarrow P$ such that $h = f$ on ∂M . Such maps always exist, but need not be unique (see e.g. [Gardiner and Lakic 2000]). On the other hand, in many circumstances there is a unique extremal map of special form which is compatible with the given boundary data. This is called a Teichmüller map, and has the desirable property of uniform conformality distortion throughout the whole domain.

Definition 2.1. The quasiconformal mapping $f : (M, g) \rightarrow (P, h)$ between Riemann surfaces is said to be *Teichmüller* provided there exists a holomorphic quadratic differential $q \in T^*M \otimes T^*M$ such that on any coordinate chart U where $q = q(z) dz^2$, the Beltrami coefficient $\mu : U \rightarrow \mathbb{C}$ satisfies

$$\mu = k \frac{\bar{q}}{|q|}, \quad k = \int_M |q| dS_g.$$

In this case, μ is said to be Teichmüller associated to f .

It is a fact that when a Teichmüller map exists, it is unique and extremal for its boundary values. Moreover, existence is guaranteed in many practically-relevant situations thanks to classical complex theory. A succinct criterion for existence in the case of surfaces with disk topology is provided by the following.

THEOREM 2.2. [Reich 2002, pg 110] Let $D \subset \mathbb{C}$ denote the closed unit disk, and suppose $g : \partial D \rightarrow \partial D$ is an orientation-preserving homeomorphism such that $dg \neq 0$ and $|\text{Hess } g| < \infty$. Then, there is a unique Teichmüller extension $f : D \rightarrow D$, $f|_{\partial D} = g$ which is extremal with respect to its boundary values.

In view of the Riemann mapping theorem, this criteria applies to any quasiconformal map $f : M \rightarrow P$ between genus zero surfaces with one boundary component. On the other hand, there is also Teichmüller existence criteria for Riemann surfaces with more general topology. In particular, given a QC map f , define the boundary dilatation of its homotopic class $[f] = \{h : M \rightarrow P : h|_{\partial M} = f|_{\partial M}\}/\sim$ as

$$H([f]) = \inf_{g \in [f]} \left\{ \inf_{C \in M} K(g|_{M \setminus C}) \right\},$$

where C is any compact set strictly contained in M . The primary existence result for Teichmüller maps in this case is due to Strebel [Strebel 1984].

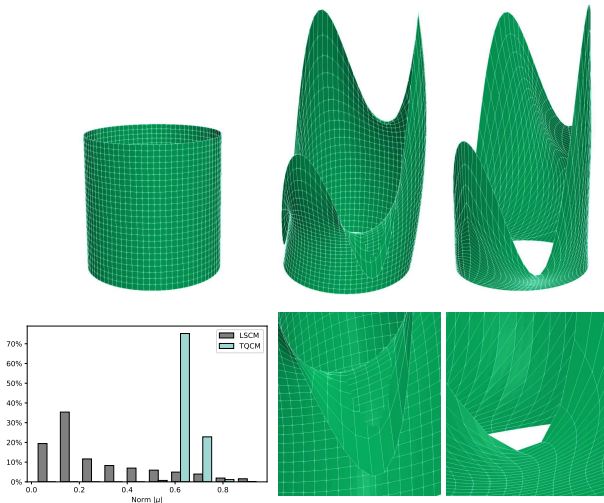


Fig. 4. Comparison of LSCM (mid) and TQCM (right) on a cylinder. Similar to the planar case, LSCM creates undesirable spillage and cannot guarantee injectivity. Conversely, TQCM remains injective despite a height distortion of 95% at the boundary.

THEOREM 2.3. [Gardiner and Lakic 2000, pg 127] Let M be a connected Riemann surface with potential boundary, and let $f : M \rightarrow f(M)$ be quasiconformal. Suppose the boundary dilatation $H([f]) < K(f)$. Then, $[f]$ contains an extremal Teichmüller mapping such that $\mu = k\bar{q}/|q|$ for some integrable holomorphic quadratic differential q . Moreover, the data (k, q) are uniquely determined up to multiplication by a positive constant.

From the above, it is clear that Teichmüller maps are remarkably well-behaved. In particular, any quasiconformal map $f : M \rightarrow P$ between Riemann surfaces satisfying “nice enough” boundary conditions contains a unique Teichmüller extremal map in its homotopic class. Conversely, it turns out that even when no extremal Teichmüller map exists, there is always a Teichmüller map with dilatation arbitrarily close to the extremal one (see [Strebel 1978, Theorem 8]). In some sense, this makes Teichmüller maps the best possible quasiconformal mappings between Riemannian surfaces M and P , and this property has generated a large amount of interest in their computation. Fortunately, Teichmüller extrema also have a deep connection to harmonic mappings which can be exploited for this purpose.

Remark 2.4. Note that the Teichmüller mappings from [Strebel 1978, Theorem 8] are allowed to be meromorphic with at most one simple pole, as opposed to purely holomorphic. This definition considerably widens the space of Teichmüller maps, at the cost of uniqueness in certain settings. Practically, QC iteration may produce mappings with the same meromorphic structure (see e.g. Figure 7).

2.2 Harmonic vs. Teichmüller

Let (M, g) be a Riemannian manifold and let J be a complex structure on TM , i.e. a linear endomorphism field such that $J^2 = -1$. Recall

that the Dirichlet energy of maps $h : (M, g) \rightarrow (\mathbb{R}^3, \delta)$ with respect to the metric $g = \sigma |dz|^2$ can be expressed locally as

$$\begin{aligned} 4\mathcal{D}_g(h) &= 2 \int_M |dh|^2 dS_g = \int_U \frac{1}{\sigma} (|\mathbf{h}_z|^2 + |\mathbf{h}_{\bar{z}}|^2) \sigma J dz \wedge d\bar{z} \\ &= 2 \int_U |\mathbf{h}_{\bar{z}}|^2 J dz \wedge d\bar{z} + \int_U (|\mathbf{h}_z|^2 - |\mathbf{h}_{\bar{z}}|^2) J dz \wedge d\bar{z} \\ &= 4C\mathcal{D}(h) + 2\mathcal{A}(h), \end{aligned}$$

where we have abused notation in the middle equalities by equating global objects to their expressions on the local domain U . Here $\mathcal{A}(h)$ is the signed area (counted with multiplicity) of the image of h , while $C\mathcal{D}(h)$ is its conformal distortion. Note that \mathcal{D}_g depends only on the metric δ of \mathbb{R}^3 and the conformal class of g , and that h is conformal if and only if $C\mathcal{D}(h) = 0$. This relationship shows that conformality is very important for harmonicity. In fact, when the target surface is fixed, the area term does not vary and so the minimizers of $C\mathcal{D}$ and \mathcal{D}_g are identical. This implies that any harmonic map is also conformal, which has proven to be quite useful for computing minimal surfaces and least-squares conformal mappings (see e.g. [Gruber and Aulisa 2020; Lévy et al. 2002; Pinkall and Polthier 1993]).

It turns out that a similar decomposition is quite useful for understanding Teichmüller quasiconformal mappings. Define the quasiconformal distortion of the mapping $h : M \rightarrow \mathbb{R}^3$ relative to the Beltrami coefficient $\mu : TM \rightarrow \mathbb{C}$ (c.f. Definition 2.8) to be

$$\begin{aligned} 4QC_\mu(h) &:= 2 \int_M |dh - \mu dh^+|^2 dS_g \\ &= \int_U \frac{1}{\sigma} |\mathbf{h}_{\bar{z}} - \mu \mathbf{h}_z|^2 \sigma J dz \wedge d\bar{z} = \int_U |\mathbf{h}_{\bar{z}} - \mu \mathbf{h}_z|^2 J dz \wedge d\bar{z}. \end{aligned}$$

As suggested by the name, $QC_\mu(h) = 0$ on any local domain U if and only if h is quasiconformal with respect to μ .

Since QC_μ measures deviation from quasiconformality, it is natural to wonder if it appears as the conformal part of some Dirichlet energy functional. To examine this, note that any mapping $f : (M, g) \rightarrow f(M) \subset (\mathbb{R}^3, \delta)$ which is quasiconformal with respect to μ induces a new metric on M , expressed locally as $g(\mu) := f^*\delta = \rho |d\zeta|^2$, where $\rho = |f_z|^2$ and $d\zeta = dz + \mu d\bar{z}$. This is simply the image metric expressed on M , which is not conformal to g unless $\mu \equiv 0$. There is then the usual notion of Dirichlet energy with respect to $g(\mu)$,

$$\begin{aligned} 4\mathcal{D}_{g(\mu)}(h) &= 2 \int_M |dh|^2 dS_{g(\mu)} = \int_U \frac{1}{\rho} (|\mathbf{h}_\zeta|^2 + |\mathbf{h}_{\bar{\zeta}}|^2) \rho J d\zeta \wedge d\bar{\zeta} \\ &= \int_U (|\mathbf{h}_\zeta|^2 + |\mathbf{h}_{\bar{\zeta}}|^2) J d\zeta \wedge d\bar{\zeta}, \end{aligned}$$

which depends on the metric δ and the conformal class of $g(\mu)$. The next result connects the critical points of $\mathcal{D}_{g(\mu)}$ to those of QC_μ in the case that μ has constant norm.

THEOREM 2.5. Let $\mu : TM \rightarrow TM$ be a Beltrami differential with constant norm $|\mu| < 1$. Then, the Dirichlet energy $\mathcal{D}_{g(\mu)}$ decomposes as

$$2\mathcal{D}_{g(\mu)}(h) = \frac{4}{1 - |\mu|^2} QC_\mu(h) + \mathcal{A}(h).$$

In particular, when the area of the image is fixed, quasiconformal maps with Beltrami coefficient μ are also harmonic with respect to the metric $g(\mu)$.

PROOF. Consider local coordinates z, \bar{z} as above so that $g = \sigma |dz|^2$, $g(\mu) = \rho |d\zeta|^2 = |\mathbf{f}_z|^2 |dz + \mu d\bar{z}|^2$. A computation establishes the Jacobian determinants

$$\begin{aligned} Jd\zeta \wedge d\bar{\zeta} &= \left(|\zeta_z|^2 - |\zeta_{\bar{z}}|^2 \right) Jdz \wedge d\bar{z} = \left(1 - |\mu|^2 \right) Jdz \wedge d\bar{z}, \\ dh \wedge d\bar{h} &= \left(|\mathbf{h}_{\zeta}|^2 - |\mathbf{h}_{\bar{\zeta}}|^2 \right) Jd\zeta \wedge d\bar{\zeta}, \end{aligned}$$

and using the representations of $d\zeta, d\bar{\zeta}$ in terms of $dz, d\bar{z}$ leads to the partial derivatives

$$\mathbf{h}_{\zeta} = \frac{1}{1 - |\mu|^2} (\mathbf{h}_z - \bar{\mu} \mathbf{h}_{\bar{z}}), \quad \mathbf{h}_{\bar{\zeta}} = \frac{1}{1 - |\mu|^2} (\mathbf{h}_{\bar{z}} - \mu \mathbf{h}_z).$$

Therefore, when μ has constant norm, the energy $\mathcal{D}_{g(\mu)}$ may be expressed as

$$\begin{aligned} 4\mathcal{D}_{g(\mu)}(h) &= \int_U 2 |\mathbf{h}_{\bar{\zeta}}|^2 Jd\zeta \wedge d\bar{\zeta} + \int_U \left(|\mathbf{h}_{\zeta}|^2 - |\mathbf{h}_{\bar{\zeta}}|^2 \right) Jd\zeta \wedge d\bar{\zeta} \\ &= \frac{2}{1 - |\mu|^2} \int_U |\mathbf{h}_{\bar{z}} - \mu \mathbf{h}_z|^2 Jdz \wedge d\bar{z} + \int_U dh \wedge d\bar{h} \\ &= \frac{8}{1 - |\mu|^2} QC_{\mu}(h) + 2\mathcal{A}(h), \end{aligned}$$

where $\mathcal{A}(h)$ is the signed area of the image surface, counted with multiplicity. Therefore, when this area is fixed $\mathcal{D}_{g(\mu)}$ and QC_{μ} have the same set of critical points. \square

Since Teichmüller mappings are unique when they exist and have Beltrami coefficients with constant norm, Theorem 2.5 implies that any homotopic class of maps from M into a fixed target which contains a Teichmüller extremum also contains a unique harmonic map, and moreover these maps coincide. Conversely, in this case it follows that minimizing QC_{μ} for a constant-norm μ is equivalent to minimizing the Dirichlet energy $D_{g(\mu)}$, which forms the basis for the QC iteration of Lui et al. [Lui et al. 2014]. Moreover, for the special case of functions $h : M \rightarrow P$ mapping M onto a compact target (P, g') with prescribed metric and everywhere non-positive Gaussian curvature, this result has an even stronger interpretation. By a theorem of Eells and Sampson (see [Eells and Sampson 1964, Section 11]), these assumptions guarantee a unique harmonic map in each homotopic class, which the previous calculation shows is also a Teichmüller mapping. Therefore, minimization algorithms (such as the QC iteration) based on this idea are guaranteed a unique global minimum, which is highly advantageous for practical computations. Indeed, it was shown in [Lui et al. 2015] that the QC iteration algorithm will converge to the unique Teichmüller extremum in this case.

On the other hand, it is desirable (and usually necessary) to apply the QC iteration algorithm in situations where there are not yet theoretical guarantees on its convergence. In particular, in remeshing applications it is not possible to control the Gaussian curvature of the target surface, and therefore the mentioned existence and uniqueness theory cannot be applied. With that said, experiments show that high-quality Teichmüller mappings are produced in these

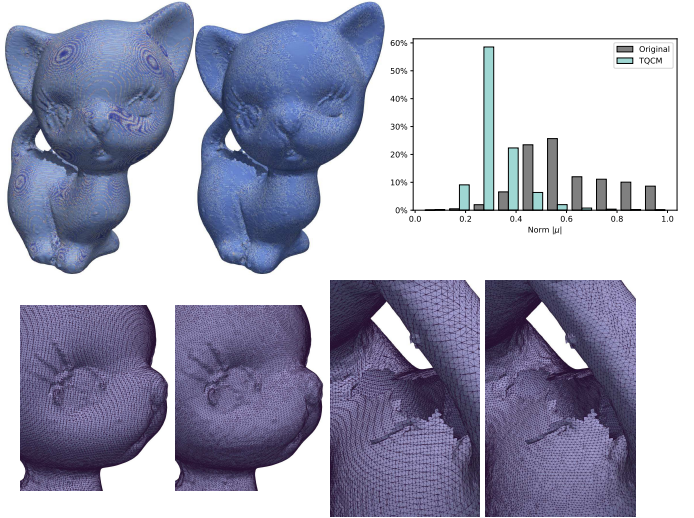


Fig. 5. Teichmüller quasiconformal remeshing of a kitten with genus 20 and many ripped edges. Note the improvement in mesh quality with TQCM despite poor initial data. (Heatmap in top row colored by $|\mu|$.)

cases as well (see e.g. Figures 1, 5, 8, 9), despite the potential lack of guaranteed behavior. To further discuss the present method for extending the QC iteration to embedded surfaces in \mathbb{R}^3 , it is necessary to recall some aspects of conformal geometry in the quaternionic setting.

2.3 Quasiconformality using Quaternions

Recall that the quaternions \mathbb{H} are the 4-dimensional division algebra over \mathbb{R} generated by the set of symbols $\{i, j, k\}$ satisfying the relations $i^2 = j^2 = k^2 = ijk = -1$. It has been shown (see e.g. [Burstall et al. 2004; Kamberov et al. 2002] and references therein) that the additional algebraic structure provided by \mathbb{H} is highly advantageous for studying the conformal geometry of immersed surfaces in a variety of settings. In particular, any immersion $f : M \rightarrow \mathbb{R}^3$ of the two-dimensional surface M can be regarded as taking values in the imaginary part of the quaternions $\text{Im } \mathbb{H}$, and therefore multiplication in \mathbb{H} (conventionally acting on the right) may be applied. This leads to a coordinate-free theory of surfaces which is adaptable, concise, and well suited for computational applications.

To illustrate some fundamental advantages of this approach, recall that $f : M \rightarrow \mathbb{R}^3$ is said to be conformal provided it maps oriented orthogonal bases of TM to oriented orthogonal bases of $df(TM)$. By standard arguments (see e.g. [Burstall et al. 2004, Lemma 2]), this implies the existence of a unit quaternion $N : M \rightarrow S^2 \subset \text{Im } \mathbb{H}$ that stabilizes $df(TM)$, i.e. such that $df(TM) = \{v \in \text{Im } \mathbb{H} \mid NvN = v\}$. Moreover, if f is oriented by a particular complex structure $J : TM \rightarrow TM$, $J^2 = \text{Id}_{TM}$, then there is only one such N compatible with the given orientation on M . It follows from these properties that the quaternion N is simply the Gauss map of the immersion f , connecting this representation to the classical theory. In fact, considering the negative Hodge star operator $*df := df \circ J$ it follows that f is conformal when and only when there exists an

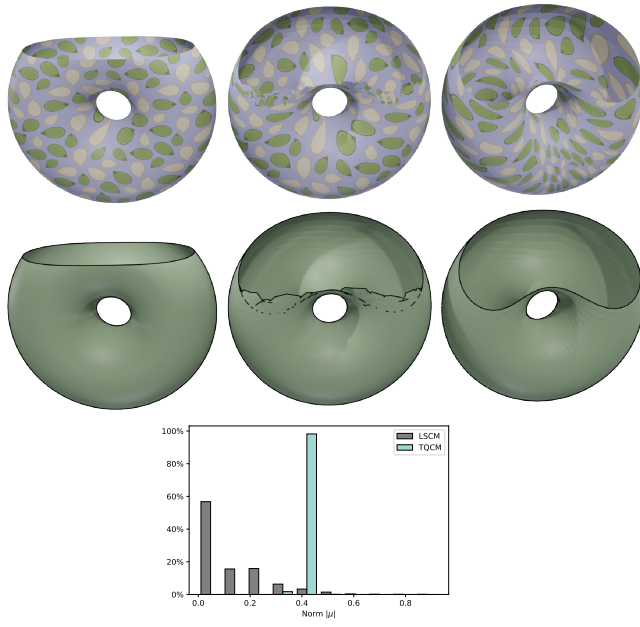


Fig. 6. Comparison of LSCM (mid) and TQCM (right) from one torus with boundary to another. Here the LSCM does not remain injective as the boundary is slid along the surface, despite its much lower average distortion.

$N : M \rightarrow S^2$ satisfying

$$*df = N df,$$

giving a definition of conformality which is independent of any metrical structure on M . This both reflects the fact that conformality is a fundamentally intrinsic notion while also enabling its manipulation through the extrinsic vector field N . As intrinsic qualities are often unwieldy in computational applications where surfaces are presented in terms of a set of extrinsic data (e.g. a list of vertex positions in \mathbb{R}^3), this connection is a major advantage of the quaternionic theory.

The next goal is to describe quasiconformality in this setting. Thankfully, there is a natural notion of complex structure (conventionally acting on the left) which is induced by the Gauss map of a conformal immersion (c.f. [Burstall et al. 2004, Section 2.1]). More precisely, given a conformal immersion $f : M \rightarrow \text{Im } \mathbb{H}$ with Gauss map $N : M \rightarrow S^2$, it is traditional to identify TM with its image $df(TM)$. In this case, using any local section $v \subset TM$ it is straightforward to check that the mapping $J : TM \rightarrow TM$ defined by

$$(a + Jb)v = va + Nvb \quad \text{for all } a + Jb \in \mathbb{C},$$

is a complex structure on TM compatible with N .

Remark 2.6. In fact, it follows that every conformal structure J on TM can be realized by the Gauss map of some conformal immersion $f : M \rightarrow \text{Im } \mathbb{H}$ (see [Kamberov et al. 2002, pg 8]). For practical computations, it is usually most convenient to employ the conformal structure which comes from the identity map $\mathbb{1}_M : M \rightarrow \mathbb{R}^3$.

Moreover, any complex structure on TM compatible with N induces a direct sum decomposition of the space $\text{Hom}(TM, \mathbb{R}^3)$ of \mathbb{R}^3 -valued one-forms analogous to classical complex theory. In particular, given $\alpha \in \text{Hom}(TM, \mathbb{R}^3)$ there are conformal resp. anticonformal parts of α with respect to f ,

$$\alpha^+ = \frac{1}{2} (\alpha - N * \alpha), \quad \alpha^- = \frac{1}{2} (\alpha + N * \alpha),$$

and it is easily checked that $*\alpha^+ = N \alpha^+$ while $*\alpha^- = -N \alpha^-$. This leads to a natural definition of quasiconformality in this setting, which enables the present extension of the QC Iteration.

Definition 2.7. Let $M \subset \mathbb{R}^3$ be an immersed surface with Gauss map $N : M \rightarrow S^2$. Then, a mapping $f : M \rightarrow \text{Im } \mathbb{H}$ is said to be quasiconformal provided there exists a measurable, \mathbb{C} -antilinear $\mu : TM \rightarrow TM$ which satisfies $|\mu|_\infty < 1$ and

$$df^- = df^+ \circ \mu,$$

with respect to the conformal structure on TM induced by N .

This is a direct analogue of the standard definition for Riemann surfaces given in Section 2.1. On the other hand, it is practically useful to rewrite the above equality using the complex structure on TM induced by N . In particular, note that the Beltrami coefficient can be interpreted as a function $\mu : TM \rightarrow \mathbb{C}$ taking values in the complex plane (or, more precisely, in the normal bundle to TM in \mathbb{H}), so that the complex-quaternionic product μdf^+ is interpreted as $(\mu df^+)(v) = \mu(v)df^+(v)$ for any section $v \subset TM$. This leads to the following equivalent to Definition 2.7. For convenience, a proof of this equivalence is given in Appendix A.

Definition 2.8. Let $M \subset \mathbb{R}^3$ be an immersed surface with Gauss map $N : M \rightarrow S^2$. Then, a mapping $f : M \rightarrow \text{Im } \mathbb{H}$ is said to be quasiconformal provided there exists a measurable, complex valued function $\mu : TM \rightarrow \mathbb{C}$ which satisfies $|\mu|_\infty < 1$ and

$$df^- = \mu df^+,$$

with respect to the conformal structure on TM induced by N .

The equality in Definition 2.8 is suggestive of the coordinate-dependent expression $f_z = \mu f_{\bar{z}}$ seen in the case of planar mappings, but has the sizeable benefit of allowing use of the quaternionic algebra outlined earlier. Note that Teichmüller immersions are defined in this setting exactly as before, and that the characteristic properties of Teichmüller Beltrami coefficients carry over as well. Therefore, the previously discussed existence theory seen in Theorem 2.2 and Theorem 2.3 applies similarly to the case of quasiconformal mappings $f : M \rightarrow \mathbb{R}^3$.

Before considering the present version of QC iteration, it is worth discussing the Beltrami coefficient $\mu : TM \rightarrow \mathbb{C}$ in greater detail. In particular, let $f : M \rightarrow \text{Im } \mathbb{H}$ be an immersion with complex structure induced by N and recall that $df = df^+ + df^-$. Then, the pullback of the metric on $f(M)$ is given by

$$f^* \delta = |df|^2 = |df^+|^2 + |df^-|^2 + 2 \operatorname{Re} (df^+ \overline{df^-}),$$

where it was used that $\langle v, w \rangle_{\mathbb{H}} = (1/2)(v\bar{w} + w\bar{v}) = \operatorname{Re}(v\bar{w})$. The $(2, 0)$ -part of this quantity is the classical Hopf differential

$Q = df^+ \overline{df^-}$ of the mapping f , which can be expressed using the definition of conformal/anticonformal parts as

$$4Q = |df|^2 - |*df|^2 - 2 \langle df, *df \rangle N.$$

Notice that this implies the Hopf differential is normal-valued, i.e. locally expressible as $Q(v) = a(v) + b(v)N$ for some smooth functions $a, b : TM \rightarrow \mathbb{R}$. Moreover, it is clear from this expression that f is conformal or anticonformal if and only if $Q \equiv 0$. Conversely, when f is quasiconformal in the sense of Definition 2.8, simple algebraic manipulations show that $Q = \bar{\mu} |df^+|^2$ or alternatively $\mu = *Q$, demonstrating that the Beltrami coefficient μ is simply the conjugate of the Hopf differential up to an application of the Hodge star. This is not surprising, since the BC μ also encodes deviation from conformality, and Teichmüller BCs were themselves defined in terms of a quadratic differential. Indeed, the structure of this object is often visible in the mapping (see e.g. Figure 7), where poles and zeroes necessarily appear according to the form of Q . Moreover, note that μ can be considered as a function which takes values in the normal bundle to the image of f in \mathbb{H} . This space is canonically isomorphic to \mathbb{C} at each point by allowing the Gauss map N to serve as the imaginary unit, in analogy with the complex structure induced by N on TM . It will now be shown that the BC μ in this setting also obeys the classical transformation rule for planar Beltrami coefficients. In particular, the quaternionic theory makes it straightforward to compute how μ behaves under a change of basis for TM .

LEMMA 2.9. *Let $a \in \mathbb{C}$ and suppose $\mu : TM \rightarrow \mathbb{C}$ is a Beltrami coefficient satisfying Definition 2.8. Then, for any local section $v \subset TM$ it follows that*

$$\mu(av) = \frac{\bar{a}^2}{|a|^2} \mu(v).$$

PROOF. Due to the conformality (resp. anticonformity) of df^+ (resp. df^-), it follows that

$$\begin{aligned} a\mu(av)df^+(v) &= (\mu df^+)(av) = df^-(av) \\ &= \bar{a}df^-(v) = \bar{a}(\mu df^+)(v) = \bar{a}\mu(v)df^+(v). \end{aligned}$$

Therefore, $\mu(v) = (a/\bar{a})\mu(av)$ and the conclusion follows. \square

In the literature on quasiconformal maps, a bounded measurable function $\mu : TM \rightarrow \mathbb{C}$ that transforms in this way is said to be a “(-1,1)-form” on TM (c.f. [Hubbard 2006, Section 4.8]). In particular, given a local coordinate z on a domain $U \subset M$, several authors write $\mu = \hat{\mu} \frac{d\bar{z}}{dz}$ for some local function $\hat{\mu} : U \rightarrow \mathbb{C}$ to illustrate the transformation rule seen in Lemma 2.9. More tensorially, any \mathbb{C} -antilinear $\mu : TM \rightarrow TM$ as in Definition 2.7 can be expressed locally as $\mu = \hat{\mu} d\bar{z} \otimes \frac{\partial}{\partial z}$, so that for any $a \in \mathbb{C}$,

$$\mu(av) = \hat{\mu} d\bar{z}(av) \otimes \frac{\partial}{\partial z} = \bar{a}\mu(v).$$

It is remarkable that the same transformation rule is readily established in the quaternionic setting without reference to any particular system of local coordinates.

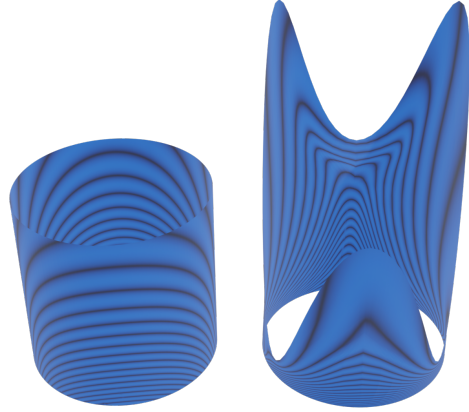


Fig. 7. Another view of the Teichmüller extremal mapping from Figure 4. Note the visible structure of the quadratic differential governing the mapping, in particular the simple pole in front and simple zero on back which “cancel out” to maintain zero Poincaré-Hopf index.

3 THE MODIFIED QC ITERATION ALGORITHM

The Quasiconformal Iteration algorithm introduced in [Lui et al. 2014] has been useful for computing extremal Teichmüller mappings between planar domains, as well as between surfaces which are conformal to planar domains. The general idea of this procedure is to find a downward trajectory toward the optimal Teichmüller map by alternately minimizing the distortion $QC_\mu(f)$ of the mapping f (for fixed μ) and the deviation of μ from Teichmüller form as defined in Definition 2.1. Under the (somewhat restrictive) assumptions mentioned in Section 2, this algorithm is guaranteed to converge to a unique Teichmüller harmonic map between any two relevant Riemann surfaces in a given homotopic class. Moreover, even when a unique Teichmüller extremum cannot be guaranteed, QC iteration should converge to something which is nearly optimal, as (meromorphic) Teichmüller mappings exist with dilation arbitrarily close to extremal.

More precisely, the QC iteration algorithm from [Lui et al. 2015, 2014] is based on the minimization of the quasiconformal distortion,

$$QC_\mu(f) = \int_M |df^- - \mu df^+|^2 dS_g,$$

which (by Theorem 2.5) is related to the conformal part of the Dirichlet energy with respect to the metric $g(\mu)$ on M . More precisely, the goal is to use minimizers of QC_μ (for fixed μ) to construct a sequence of Beltrami coefficients $\{\mu_k\}_{k=0}^N$ which converges to a coefficient μ_N which is approximately Teichmüller, i.e. approximately satisfies Definition 2.1. Accomplishing this requires an efficient way to compute quasiconformal mappings f given μ and vice versa, along with a procedure which encourages μ to have the correct local structure at each iteration. The planar technology for doing this was developed in [Lui et al. 2014], and the remainder of the present work is devoted to adapting these ideas to the more general setting of immersed surfaces in \mathbb{R}^3 . Although originally formulated in terms of mappings between fixed Riemann surfaces (M, g) and (N, h) , it turns out that the QC Iteration is still useful in settings

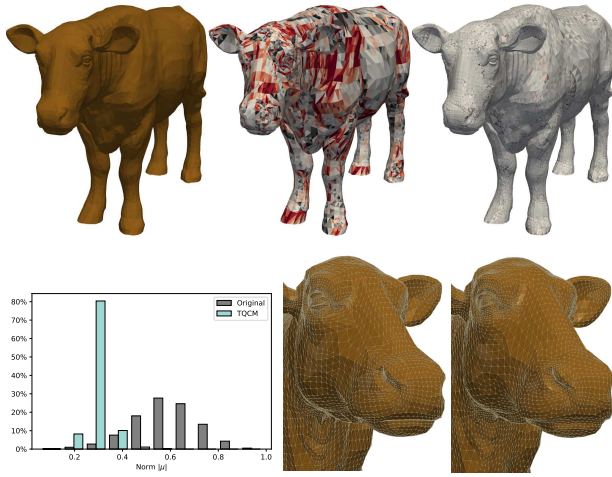


Fig. 8. Remeshing of a cow with genus 0. The histogram shows that a high quality approximate Teichmüller mapping is produced despite the fact that any such mapping cannot be extremal in this case. (Heatmap in top row colored by $|\mu|$).

where the target $f(M)$ is a surface in \mathbb{R}^3 with metric $f^*\delta$ determined by the mapping itself. In fact, the quaternionic technology from the last Section enables the modified QC iteration procedure outlined in Algorithm 3, which directly computes a Teichmüller quasiconformal mapping $f : M \rightarrow \mathbb{R}^3$ satisfying prescribed Dirichlet boundary data. The remainder of this Section discusses each step of the algorithm in detail.

Algorithm 1 High-level description of the QC iteration

Require: Surface $M \subset \mathbb{R}^3$. Beltrami coefficient $\mu_0 = 0$. Stopping tolerance $\varepsilon > 0$ and maximum iteration number N .

for integer $0 \leq k \leq N$ **do**

- while** $QC_{\mu_k}(f_k) > \varepsilon$ **do**
- (1) Compute $f_k : M \rightarrow \mathbb{R}^3$ given μ_k .
- (2) Compute v_{k+1} given f_k .
- (3) Post-process v_{k+1} to bring it closer to Teichmüller form, generating ξ_{k+1} .
- (4) Minimize $QC_{\mu}(f_k)$ on the line between μ_k and ξ_{k+1} , generating μ_{k+1} .
- end while**
- end for**

3.1 Step 1: Computing Quasiconformal Mappings

Given a Beltrami coefficient $\mu : TM \rightarrow \mathbb{C}$, it is necessary to compute a corresponding quasiconformal mapping $f : M \rightarrow \mathbb{R}^3$. More precisely, if $M \subset \mathbb{R}^3$ and $N : M \rightarrow S^2$ are given, then N defines a complex structure on M as before and it is meaningful to consider the quasiconformal distortion QC_{μ} of mappings from M . For the purposes of QC iteration, it is sufficient that $f : M \rightarrow \mathbb{R}^3$ be quasiconformal with BC μ in a least-squares sense. In particular, a

function is sought which solves the problem

$$\min_f QC_{\mu}(f), \quad f|_{\partial M} = u,$$

in a fixed homotopic class and where $u : \partial M \rightarrow \mathbb{R}^3$ is a prescribed function representing the desired boundary data. Expressing f in terms of a one-parameter family of mappings $f(x, t) = f(x) + t\varphi(x)$ for $t \in (-\varepsilon, \varepsilon)$ and some variation $\varphi : M \rightarrow \mathbb{R}^3$, standard techniques from the calculus of variations yield a necessary criterion for f to be a minimizer of QC_{μ} . In particular, using the fact that μ , the conformal structure, and the metric on M are fixed, the derivative of the functional QC_{μ} at f in the direction φ is given by

$$\begin{aligned} \delta QC_{\mu}(f)\varphi &:= \frac{d}{dt} \Big|_{t=0} QC_{\mu}(f + t\varphi) \\ &= \int_M \langle df^- - \mu df^+, d\varphi^- - \mu d\varphi^+ \rangle \, dS_g, \end{aligned}$$

which can be discretized and solved using e.g. finite element methods. Moreover, by standard elliptic theory, the f which minimizes the above will necessarily be a local minimizer of the quasiconformal distortion, if not a true quasiconformal mapping. Therefore, the mapping f which minimizes this quantity for all admissible variations φ is then taken to be the output to Step 1 of the algorithm.

Remark 3.1. For remeshing applications, it is desirable that the Dirichlet data $u : \partial M \rightarrow \mathbb{R}^3$ coincide with the identity mapping $\mathbb{1}_{\partial M}$ on the boundary. Since boundary nodes in the discrete setting are fixed *a priori*, this illustrates the appeal of optimizing the quasiconformal distortion as opposed to the conformal distortion ($\mu \equiv 0$ in the above), since there is likely no conformal mapping satisfying the given boundary condition.

Clearly, the f satisfying the above minimization is not guaranteed to preserve the extrinsic geometry of M in \mathbb{R}^3 . Therefore, it is useful to consider a shape-preserving variant which is suitable for producing mappings which satisfy given boundary conditions while also remaining close to the reference immersion. Particularly when remeshing, a map $f : (M, g) \rightarrow (M, g(\mu))$ is desired which optimizes mesh element angles while preserving the Gauss map N as well as possible. Accomplishing this within the context of the QC iteration requires a constraint that can be enforced during the minimization of the quasiconformal distortion functional. One effective option for this has been examined in [Gruber and Aulisa 2020] for the purposes of preserving extrinsic features while minimizing the conformal distortion. More specifically, consider a point $x \in M$, an immersion $f : M \rightarrow \mathbb{R}^3$, and a curve $f(x + tv)$ for some $v \in TM$ and $0 \leq |t| < T$. Then, this curve lies on the immersed surface $f(M)$, and if N is normal to this surface then Taylor expansion around $t = 0$ shows

$$\begin{aligned} f(x + tv) &= f(x) + t df_x(v) + \frac{t^2}{2} (\nabla df)_x(v, v) + O(t^3), \\ N\left(x + \frac{t}{2}v\right) &= N(x) + \frac{t}{2} dN_x(v) + O(t^2). \end{aligned}$$

Moreover, since $\langle N, df(v) \rangle = 0$ (pointwise) for all $v \in TM$, differentiation yields that

$$\langle dN(v), df(v) \rangle + \langle N, (\nabla df)(v, v) \rangle = 0.$$

Therefore, it follows that

$$\left\langle f(\mathbf{x} + t\mathbf{v}) - f(\mathbf{x}), N \left(\mathbf{x} + \frac{t}{2}\mathbf{v} \right) \right\rangle = 0 + O(t^3),$$

and so the inner product of the difference vector $f(\mathbf{x} + t\mathbf{v}) - f(\mathbf{x})$ with the normal vector in the middle vanishes to third order.

This inspires a constraint for shape-controlled minimization of QC_μ . In particular, to keep the image of f close to the reference immersion $\mathbb{1}_M$ it is reasonable to require that

$$\langle f(\mathbf{x}) - \mathbb{1}_M(\mathbf{x}), N_{mid}(\mathbf{x}) \rangle = 0,$$

where $N_{mid} = (1/2)(N_{old} + N_{new})$ approximates the normal halfway between the image of $\mathbb{1}_M$ and the image of f . In remeshing applications, this ensures that the difference vectors between the current and new points on M remain orthogonal to the normal vectors in between, yielding a constraint which can be readily discretized and implemented along with the minimization of QC_μ as a Lagrange multiplier. In particular, consider the problem of finding a pair of functions $v : M \rightarrow \mathbb{R}^3$ and $\rho : M \rightarrow \mathbb{R}$ which satisfy

$$\min_v \left(QC_\mu(\mathbb{1}_M + v) + \frac{\epsilon}{2} \int_M \rho^2 dS_g + \int_M \rho \langle v, N \rangle dS_g \right),$$

where $\epsilon > 0$ is a fixed penalty parameter and $v|_{\partial M} = 0$. Then, $f = \mathbb{1}_M + v$ minimizes QC_μ and satisfies the desired constraint. Formulated weakly, desired pair v, ρ should satisfy the system

$$\begin{aligned} 0 &= \int_M \rho \langle \varphi, N \rangle dS_g + \delta QC_\mu(\mathbb{1}_M + v) \varphi, \\ 0 &= \int_M \psi \langle v, N \rangle dS_g + \epsilon \int_M \psi \rho dS_g, \end{aligned} \quad (1)$$

for all suitable variations $\varphi : M \rightarrow \mathbb{R}^3$ and $\psi : M \rightarrow \mathbb{R}$. The mapping $f = \mathbb{1}_M + v$ which minimizes this modified problem is then a suitable remeshing of the original surface M . Indeed, Figures 9 and 8 show that this procedure is suitable for preserving extrinsic features even around corners and delicate contours in the mesh such as facial expressions.

Remark 3.2. Here, the penalty parameter $\epsilon \approx 10^{-5}$ is used to ensure L^2 -regularity for the Lagrange multiplier ρ .

3.2 Step 2: Computing the Beltrami Coefficient

Once a particular quasiconformal mapping $f : M \rightarrow \mathbb{R}^3$ has been determined, it is necessary to compute its Beltrami coefficient v in the complex structure determined by N . Here illustrates a huge benefit of the quaternionic theory seen before. Precisely, since $\mathbb{R}^3 \cong \text{Im } \mathbb{H}$, computing the desired function $v : TM \rightarrow \mathbb{C}$ as in Definition 2.8 becomes a simple algebraic exercise.

LEMMA 3.3. Let $f : M \rightarrow \text{Im } \mathbb{H}$ be a quasiconformal mapping with respect to the complex structure induced by $N : M \rightarrow S^2$. Then, the Beltrami coefficient $\mu : TM \rightarrow \mathbb{C}$, $\mu = \mu^1 + J\mu^2$ can be expressed component-wise as

$$\mu^1 = \text{Re} \left(\frac{df^- \overline{df^+}}{|df^+|^2} \right), \quad \mu^2 = \text{Re} \left(\frac{df^- \overline{N df^+}}{|df^+|^2} \right),$$

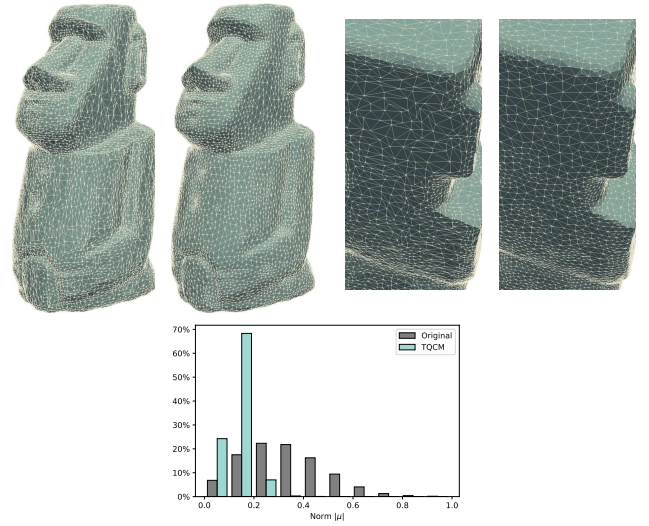


Fig. 9. Remeshing of a moai statue. Note that the minimization constraint preserves extrinsic features with only minimal rounding of the corners.

PROOF. Since $df^- = \mu df^+$, the definition of the complex structure on TM induced by N yields

$$\frac{df^- \overline{df^+}}{|df^+|^2} = \mu(1) = \mu^1 + \mu^2 N.$$

The desired representation now follows from the fact that $\overline{vw} = \overline{w}\overline{v}$ for quaternions $v, w \in \mathbb{H}$. \square

This Lemma provides a quick and straightforward way to extract the Beltrami coefficient of the least-squares minimizer from Step 1 of the QC iteration. On the other hand, recall that the components of μ are not invariant under changes of basis for TM . In particular, once a local section $v = v^i \partial_i$ of TM is chosen (say on a particular mesh element), this computation gives the components of $\mu = \mu(v)$ relative to that particular choice. This is the analog of coordinate dependence for Beltrami coefficients $\mu : TM \rightarrow \mathbb{C}$, which is captured in Lemma 2.9.

3.3 Step 3: Post-processing the Beltrami Coefficient

Once the Beltrami coefficient v has been computed from the most recent minimizer $f : M \rightarrow \mathbb{R}^3$, it is smoothed and projected in order to bring it closer to Teichmüller form. More precisely, a composition of local Laplace smoothing on v along with projection onto the space of constant-norm BC's is performed in order to yield a new BC ξ which is closer to optimal with respect to its local structure. To describe this in more detail, note the following result.

LEMMA 3.4. Any Teichmüller Beltrami coefficient $\mu = \mu^1 + J\mu^2$ has harmonic norm, as well as harmonic argument. Conversely, any pair (k, θ) where $k \in \mathbb{R}$ and $\Delta\theta = 0$ can be associated with a Teichmüller Beltrami coefficient $\mu : TM \rightarrow \mathbb{C}$.

PROOF. Recall that on any coordinate patch U the Teichmüller Beltrami coefficient satisfies

$$\mu = k \frac{\bar{q}}{|q|},$$

where $k \in \mathbb{R}$ and q is a local holomorphic function. Therefore, it follows immediately that the norm is constant, hence harmonic. Moreover, since q is holomorphic, so is $\log q = \log |q| + J \arg q$ (in an appropriate branch) and it follows that $\arg q$ is harmonic also. Finally, we have

$$e^{J \arg \mu} = \frac{\bar{q}}{|q|},$$

so that $\arg \mu = -\arg q$ which implies the first conclusion. Conversely, if θ is a harmonic function, then there is a conjugate harmonic function ϕ so that $\phi - J\theta$ is holomorphic. In this case, $q = e^{\phi - J\theta}$ is also holomorphic and

$$\mu = |\mu| e^{J\theta} = k \frac{\bar{q}}{|q|}$$

is Teichmüller. \square

By the Lemma, the optimal BC μ should have constant norm and harmonic argument as functions on M . However, it is not *a priori* clear what values they should take. Therefore, the next step in the QC iteration is to perturb the current BC v in a way that brings its local structure closer to optimal. This involves first averaging the complex phase $e^{J \arg v}$ of the BC v in a neighborhood of each mesh element, which (gently) diffuses this quantity over the surface and moves v in the direction of a Teichmüller BC. The details of this procedure are postponed to Section 4, as they rely on the discretization of the surface M . On the other hand, this averaging can be formally represented by an operator \mathcal{S} , so that

$$\mathcal{S}(e^{J \arg v}) = e^{J \arg \xi},$$

defines the phase of a new BC ξ . This is one half of a polar decomposition which defines the post-processed BC ξ . The norm $|\xi|$ is then obtained by projecting v onto the space of constant-norm Beltrami coefficients. Since the appropriate constant is not known, a reasonable choice for the target norm is the average value of $|v|$ integrated over the source surface, leading to the equality

$$|\xi| = \frac{\int_M |v| dS_g}{\int_M dS_g}.$$

From this information, it is easy to reconstruct the post-processed BC as $\xi = |\xi| e^{J \arg \xi}$, yielding a constant-norm object which is closer to Teichmüller as defined by Definition 2.1. Moreover, note that this local averaging will affect neither $|v|$ nor $\arg v$ in the event that v is already optimal and M is simply connected. Indeed, the former statement is clear from the fact that a Teichmüller $|v|$ is constant, while the latter follows from $\Delta e^{J\theta} = e^{J\theta} (J\Delta\theta - |\nabla\theta|^2)$ which vanishes for harmonic θ on simply connected M . Although it is not necessarily true that $\nabla\theta = 0$ in the higher-genus case, Step 4 ensures that ξ is chosen only if it does not increase the distortion QC_μ .

Remark 3.5. The smoothing proposed in [Lui et al. 2014] is done directly on the argument $\arg v$ instead of the phase $e^{J \arg v}$. However, this still has the potential to cause drift away from the Teichmüller

optimum in the multiply-connected case, and we observe better results by smoothing on the phase regardless of the underlying topology of the surface. As the local averaging is done only once per iteration with the goal of perturbing the BC, this does not hinder the algorithm in practice.

3.4 Step 4: Ensuring the Distortion is Non-increasing

The final step in the present algorithm is to ensure that the quasiconformal distortion QC_μ does not increase during the k^{th} iteration of this process. This is done by searching for the energetically optimal Beltrami coefficient on the straight line between μ_k and ξ_{k+1} . In particular, consider the linear combination $\mu(t) = t\mu_k + (1-t)\xi_{k+1}$ of the BC μ_k from the beginning of iteration stage k and the smoothed BC ξ_{k+1} from the last step. Then, using $\dot{\mu} = \mu_k - \xi_{k+1}$ to denote differentiation with respect to t , the derivative of $QC(f_k)$ is given by

$$\dot{QC}_\mu(f_k) = \int_M \langle \dot{\mu} df_k^+, df_k^- - \mu df_k^+ \rangle dS_g.$$

Therefore, $\dot{QC}_\mu(f_k) = 0$ precisely when

$$t_0 = \frac{\int_M \langle \dot{\mu} df_k^+, df_k^- - \xi_{k+1} df_k^+ \rangle dS_g}{\int_M |\dot{\mu} df_k^+|^2 dS_g},$$

yielding the optimal BC along this linear interpolation. With this, choosing $t = t_0$ produces the updated Beltrami coefficient $\mu_{k+1} = \mu(t_0)$ used for the next iteration.

Remark 3.6. It is worth mentioning that Step 4 is not present in the original formulation of [Lui et al. 2014], and is not strictly necessary for the QC iteration to be applied. On the other hand, faster convergence and better overall performance is observed when it is included.

4 DETAILS OF THE DISCRETIZATION

Now that the present version of the QC iteration has been discussed in detail, it is pertinent to discuss the discretization of the relevant systems. It is assumed that the source surface $M = M_h$ is given as a structured or unstructured orientable manifold mesh of triangles or quadrilaterals which are not degenerate. Note that this implies that the interior angles of each element must be bounded below, although this bound may be very close to zero in practice as in the case of Figures 1 and 5. Under this assumption, M_h can be expressed as the union

$$M_h = \bigcup_{T_h \in \mathcal{T}_h} T_h,$$

where each T_h is an element of the discrete surface. Additionally, it will be assumed that the vertices of M_h are embedded in \mathbb{R}^3 , so that $M_h \subset \mathbb{R}^3$ carries a submanifold structure via the usual identity mapping $\mathbb{1}_{M_h} : M_h \rightarrow \mathbb{R}^3$. In practice, it is convenient to coordinatize M_h with local parametrizations $X_h : U_h \rightarrow M_h$ so that each element T_h lies in the image of (at least one) X_h . This implies that functions on M_h may be discretized using a piecewise-linear basis supported on each element (see e.g. [Dziuk and Elliott 2013]). In particular, if the vertices of M_h are denoted by $\{v_j\}_{j=1}^{N_v}$, the standard Lagrange nodal basis $\{\phi_i\}_{i=1}^N$ on M_h satisfies $\phi_i(v_j) = \delta_{ij}$. The space

of piecewise-linear finite elements on M_h is then

$$S_h = \text{Span}\{\phi_i\} = \{\phi \in C^0(M_h) : \phi|_{T_h} \in \mathbb{P}_1(T_h), T_h \in \mathcal{T}_h\},$$

where $\mathbb{P}_1(T_h)$ denotes the space of linear polynomials on T_h . Of course, the appropriate objects on U_h are defined by simply pulling back these quantities along the parametrization X_h .

4.1 Local Expressions

To carry out the QC iteration in this framework, it is necessary to have local expressions for the functionals discussed in Section 3. To that end, suppose the smooth surface M is coordinatized by local parametrizations, each of which looks like $X : U \rightarrow M$ for some domain $U \subset \mathbb{R}^2$ (see Figure 10). It follows that if $\{x^1, x^2\}$ are coordinates on U , then $\{\partial_1, \partial_2\}$ form the standard basis for TU where $\partial_i := \partial/\partial x^i$. Moreover, using the dual basis defined by $dx^i(\partial_j) = \delta_j^i$ the differential of X has the expression $dX = X_i \otimes dx^i$ (Einstein summation assumed) where

$$X_i = X_i^j \partial_j, \quad X_i^j = \frac{\partial X^j}{\partial x^i}.$$

Clearly, this coordinate representation of X lies on the abstract surface M and need not exist in \mathbb{R}^3 . On the other hand, post-composition with the identity map $\mathbb{1}_M : M \rightarrow \mathbb{R}^3$ yields an equivalent mapping $\mathbb{1}_M \circ X = X$, so that the vectors X_i have the alternative expression in terms of the standard basis $\{\mathbf{e}_I\}$ for \mathbb{R}^3 ,

$$X_i = X_i^J \mathbf{e}_J, \quad X_i^J = \frac{\partial X^J}{\partial x^i}.$$

This identification yields a local expression on U of the Riemannian metric g on $M \subset \mathbb{R}^3$, given component-wise as $g_{ij} = \langle X_i, X_j \rangle$. Similarly, the area element on M becomes $dS_g = \sqrt{\det g} dx^1 \wedge dx^2$, and the (outward-directed) unit normal field to M is readily expressed as

$$N = \frac{\mathbf{X}_1 \times \mathbf{X}_2}{|\mathbf{X}_1 \times \mathbf{X}_2|}.$$

With this, any function $f : M \rightarrow \mathbb{R}^3$ can be treated as a function on U through the pullback $F = f \circ X$, so that its differential becomes

$$df = \mathbf{F}_i \otimes \omega^i = g^{ij} \mathbf{F}_i \otimes \mathbf{X}_j,$$

where $\{\omega^i\}$ is the dual basis to $\{X_i\}$ and g^{ij} are the components of the metric inverse defined by $g^{ik} g_{kj} = \delta_j^i$. The vector fields $\mathbf{F}_i = df(X_i) = d(f \circ X)(\partial_i)$ are then expressed in terms of the same basis $\{\mathbf{e}_I\}$,

$$\mathbf{F}_i = F_i^J \mathbf{e}_J, \quad F_i^J = \frac{\partial (f \circ X)^J}{\partial x^i},$$

which yields a local expression for (twice) the Dirichlet energy density of f ,

$$|df|^2 = g^{ij} \langle \mathbf{F}_i, \mathbf{F}_j \rangle = g^{ij} \delta_{IJ} F_i^I F_j^J.$$

This allows for a local expression of the quasiconformal distortion functional QC_μ . Suppose the Beltrami coefficient $\mu : TU \rightarrow \mathbb{C}$ is specified as a value per element $\mu_F := \mu(\partial_1)$. Then, it follows that

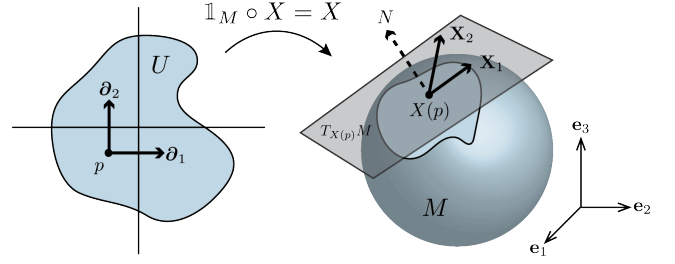


Fig. 10. The parametrization X coordinatizes a portion of the surface M . The vector fields ∂_i form a basis for $T_p U$, while their images $\mathbf{X}_i = dX(\partial_i)$ form a basis for $T_{X(p)} M$.

$\mu(\partial_2) = -\mu(\partial_1) = -\mu_F$ (easily checked with Lemma 2.9) and there are the coordinate expressions

$$\begin{aligned} (Q_1 f^I) \mathbf{e}_I &:= dF^-(\partial_1) - \mu(\partial_1) dF^+(\partial_1) \\ &= \left((1 - \mu_F) F_1^I + (1 + \mu_F) N F_2^I \right) \mathbf{e}_I, \\ (Q_2 f^I) \mathbf{e}_I &:= dF^-(\partial_2) - \mu(\partial_2) dF^+(\partial_2) \\ &= \left((1 + \mu_F) F_2^I - (1 - \mu_F) N F_1^I \right) \mathbf{e}_I. \end{aligned}$$

Note the presence of complex and quaternionic products in the above which must be attended to during the implementation. Using $\langle a, b \rangle = \text{Re}(ab)$ along with $\overline{ab} = \bar{b}\bar{a}$ and the fact that the \mathbf{e}_I are pure imaginary, it follows that

$$\begin{aligned} |df^- - \mu df^+|^2 &= g^{ij} \langle (Q_i f^K) \mathbf{e}_K, (Q_j f^L) \mathbf{e}_L \rangle \\ &= -g^{ij} \text{Re} \left(Q_i f^K \mathbf{e}_{K \times L} \overline{Q_j f^L} \right), \end{aligned}$$

where $\mathbf{e}_{K \times L} = \mathbf{e}_K \times \mathbf{e}_L$ when $K \neq L$ and 1 otherwise. Putting this together, the quasiconformal distortion of the local image $(f \circ X)(U)$ has the representation

$$\begin{aligned} QC_\mu(f) &= \int_U |df^- - \mu df^+|^2 dS_g \\ &= \int_U -g^{ij} \text{Re} \left(Q_i f^K \mathbf{e}_{K \times L} \overline{Q_j f^L} \right) \sqrt{\det g} dx^1 \wedge dx^2. \end{aligned}$$

Of course, the quasiconformal distortion of the mapping f on the entirety of M is easily recovered as the sum of these local contributions.

4.2 Minimizing Quasiconformal Distortion

With local expressions available, it is now straightforward to implement the minimization of QC_μ in Section 3.1. On the other hand, the results of this procedure are dependent on the shape of the reference elements used to represent (the local preimages of) M_h , so it is important to discuss how these elements are chosen in practice. First, notice that on each reference domain U_h the discretized functional QC_μ will measure the μ -quasiconformal distortion of a mapping $f \circ X_h : U_h \rightarrow \mathbb{R}^3$ with respect to a particular discretization of U_h . In particular, the deviation from μ -quasiconformality will be reflected in the way mesh elements are distorted as they move from U_h into

\mathbb{R}^3 under this mapping, so it is important to specify a configuration on U_h to which the target surface should be quasiconformal. One obvious choice for this comes from pulling back the initial triangulation/quadrangulation of M_h onto the reference domains U_h . However, it is often the case that angles coming from the initial configuration are nearly degenerate (see e.g. Figure 5 and Figure 1), so this choice is not useful if the goal is to improve the mesh on the surface. Besides this, the identity mapping is always conformal (hence quasiconformal) with distortion zero, so in fact this choice will not re-mesh the surface at all. Another possibility for the reference discretization is to require the interior angles to be as close as possible to $\pi/3$ in triangular elements and $\pi/2$ for quadrangular elements. But this choice can also lead to a poor discretization for unstructured meshes, as vertices of the surface M_h may lie on a variable number of elements.

In contrast to the above approaches, the present implementation uses the “optimized” Algorithm 2 to determine shape of each reference element. Inspired by the idea of conformal flatness, this procedure chooses interior angles in such a way that each vertex of M_h has ideal exterior angles which sum to 2π . To describe this in more detail, consider that any vertex v_i away from the boundary is surrounded by a fixed number of elements m_i , and for each element containing v_i it is desirable for the corresponding interior angle α_i to be as close as possible to $2\pi/m_i$. Moreover, the sum of the interior angles α_i in each element should equal π or 2π for triangular or quadrilateral elements, respectively. Therefore, if a leading node v_i exists in an element such that $\alpha_i > \alpha_j$ for all $j \neq i$, then we fix α_i and redistribute the remaining angle sum $\pi - \alpha_i$ (or $2\pi - \alpha_i$ for quadrilateral elements) to the other nodes v_j proportionally to the value of α_j . If a leading node does not exist in a particular element, then we redistribute the angle sum π (or 2π for quadrilateral elements) to all nodes v_j proportionally to the value of α_j .

Once the angles are found we reconstruct the reference triangle and quadrilateral satisfying the following constraints. For the triangle: the first vertex is at $(-0.5, 0)$, the second vertex is on the x_1 -axis on the right of the first one, and the area is $\sqrt{3}/4$. For the quadrilateral: the first vertex is at $(0, 0)$, the second vertex is on the x_1 -axis on the right of the first one, the area is 1, and the quadrilateral circumscribes a circle. The last constraint ensures that the summed lengths of opposite sides will be equal. For equal angle configurations, these correspond to an equilateral triangle of side 1 and to a square of side 1, respectively.

Once the reference elements have been constructed, any function $f : M_h \rightarrow \mathbb{R}^3$ can be represented component-wise in the nodal basis for U_h as $f^K = F_\alpha^K \varphi^\alpha$. Here $F_\alpha^K = (f \circ X)_\alpha^K$ denotes the value of the K^{th} component at node α and $\varphi = \phi \circ X$ satisfies $\varphi^\alpha(v_\beta) = \delta_{\beta}^\alpha$. It follows that the derivative of f^K in the direction X_i is then $F_i^K = F_\alpha^K \varphi_i^\alpha$, so that the minimization of $QC_\mu(f)$ can be expressed as the linear system ($U = \cup U_h$)

$$\begin{aligned} \mathcal{R}(QC_\mu)^{K\beta} &:= \delta QC_\mu(f^K) \Phi^\beta \\ &= F_\alpha^K \int_U -g^{ij} \operatorname{Re} \left(Q_i \varphi^\alpha \mathbf{e}_{K \times L} \overline{Q_j \varphi^L} \right) \sqrt{\det g} dA \\ &=: F_\alpha^K \mathcal{T}(QC_\mu)^{\alpha\beta}, \end{aligned}$$

Algorithm 2 Generation of reference angles

Require: Reference triangulation \mathcal{T} of the closed surface M .

```

for  $T \in \mathcal{T}$  do
    if  $T$  is triangle then
         $N_T = 3, \Theta = \pi$ 
    else if  $T$  is quadrilateral then
         $N_T = 4, \Theta = 2\pi$ 
    end if
    for vertex  $1 \leq i \leq N_T$  do
        Compute  $m_i = \#$  of adjacent elements
         $\alpha_i \leftarrow 2\pi/m_i$ 
    end for
    Determine maximum vertex angle  $\alpha_i$ .
    if  $\alpha_i > \alpha_j$  for all  $j \neq i$  then
         $\beta_i = \alpha_i$ 
        for vertices  $j \neq i$  do
             $\beta_j = \alpha_j (\Theta - \alpha_i) / (\sum_{k \neq i} \alpha_k)$ 
        end for
    else
        for vertices  $1 \leq j \leq N_T$  do
             $\beta_j = \alpha_j \Theta / \left( \sum_{k=1}^{N_T} \alpha_k \right)$ 
        end for
    end if
end for
return  $\beta$ 

```

where $\mathcal{J}(QC_\mu)$ is the Jacobian operator of the system and $\mathcal{R}(QC_\mu)$ is the residual. Note that $\Phi^\beta = \varphi^L \beta$ is simply three independent copies of the nodal vector φ^β . With this, the discrete version of the linear system (1) is straightforward to implement. In practice, μ was identified with the normal-valued quaternionic function $\mu^1 + \mu^2 N$ and the Boost library [Schäling 2011] was used to compute the relevant quaternion products. The examples from this paper were implemented in the open source finite element library FEMuS [Aulisa et al. 2014].

4.3 Smoothing the Norm and Phase of the BC

It remains to discuss the particular smoothing operation which was denoted \mathcal{S} in Step 3 of the algorithm and is illustrated in Figure 11. First, recall that the BC $\mu = \mu_F$ is stored as a per-element value (on M_h) which is aligned with the basis vector ∂_1 coming from the bottom edge of the reference element (on U_h). From this data, it is easy to extract the polar decomposition $\mu_F = |\mu_F| e^{j \arg \mu_F}$ which gives the norm and local argument of μ_F . The averaging operations on the norm and the argument are then performed separately. As mentioned in 3, the norm of the BC is made constant so as to replicate the behavior of the Teichmüller optimum. In practice, this means computing the average of the norm on the faces

$$|\mu|_{avg} = \frac{1}{N_{el}} \sum_{F=1}^{N_{el}} |\mu_F|,$$

which then replaces the value of $|\mu|$ on every face of the mesh.

The local smoothing operation on the phase $e^{J \arg \mu_F}$ is more delicate due to the basis-dependence of μ . Consider a reference element on the parametrization domain U_h with basis vector ∂_1 aligned with its bottom edge. Then, an adjacent edge making an angle θ with the bottom edge carries a natural direction vector given by $e^{J\theta}\partial_1 = \cos\theta\partial_1 + J\sin\theta\partial_1$. Note that unless the image of this adjacent edge lies on the boundary, there is some other element of M_h which shares it, and (as the mesh is unstructured) the preimage of this element may or may not share the direction ∂_1 . Therefore, it is not sufficient to average the representations $\mu = \mu(\partial_1)$ directly, as there is no guarantee that the basis vectors of neighboring elements are properly aligned. On the other hand, it follows from Lemma 2.9 that the Beltrami coefficient on the edges of any element is computable from $\mu(\partial_1)$, i.e. if $a = e^{J\theta}$ then $\mu(a\partial_1) = e^{-2J\theta}\mu(\partial_1)$. Therefore, a local averaging operation S is still feasible as long as the values of μ are aligned beforehand. Moreover, it is easy to see that the reflection $a\partial_1 \mapsto -a\partial_1$ induces no change in μ , so that the values of μ on shared edges (necessarily oriented oppositely) will be component-wise comparable. Therefore, smoothing on the phase of μ involves first projecting $e^{J \arg \mu_F} = \mu_F / |\mu_F|$ to the edges, averaging their values there, and then re-projecting these averaged values back into the faces. More precisely, consider an element F and the positive angle $\theta_i = \angle(e_1, e_i)$ which each edge e_i of F makes with edge 1. Then, the projection from F to its edges is built as

$$P(\theta_i) = \begin{pmatrix} \cos^2 \theta_i - \sin^2 \theta_i & -2\cos \theta_i \sin \theta_i \\ 2\cos \theta_i \sin \theta_i & \cos^2 \theta_i - \sin^2 \theta_i \end{pmatrix},$$

so that $\mu_i := P(\theta_i)\mu$ gives the appropriate value of μ on the i^{th} edge of F . Doing this over all elements $1 \leq F \leq N_{el}$ gives the per-edge values $\mu_{F,i}/|\mu_F|$ corresponding to the phases $e^{J \arg \mu_{F,i}}$ that can be averaged according to how many elements share each edge. In particular, since reversing the orientation of an edge does not change the value of the phase, it suffices to add the contributions of each local edge $\mu_{F,i}/|\mu_F|$ to the global edge phase $e^{J \arg \mu_\alpha}$, $1 \leq \alpha \leq N_{edges}$, and then divide by the number of elements sharing edge α . Note that the number of elements sharing each edge α is either 1 or 2, for boundary or internal edges, respectively. This action yields a smoothed μ phase in each edge, which can be averaged back from the edges to the faces with $P^T(\theta_i)$. Finally, once the norm and the phase of μ_F have been independently averaged, the new BC (denoted ξ in Section 3) on the face F is reconstructed as

$$\xi_F = |\mu|_{avg} S(e^{J \arg \mu_F}),$$

where S denotes the local smoothing operation just discussed. Pseudocode for this procedure is given in Algorithm 3.

5 CONCLUSIONS AND FUTURE WORK

An algorithm has been presented for computing Teichmüller quasiconformal mappings from immersed surfaces in Euclidean space. Building on the idea of QC iteration, this procedure has been shown to produce mappings with approximately uniform conformality distortion throughout their domain, which are useful for interpolating fixed boundary conditions and producing optimal surface meshes with specified element connectivity. However, there remain several challenges and avenues for future work in this area. One very basic

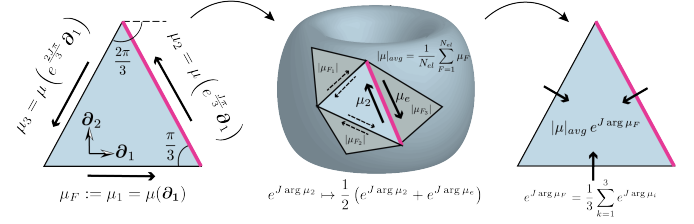


Fig. 11. Step 3 of the QC iteration in the discrete setting applied to a triangular element with equal reference angles. Here the local averaging of the norm and phase are illustrated. The post-processed BC on each element is reconstructed as $\mu = |\mu| e^{J \arg \mu}$.

Algorithm 3 Post-processing of μ_F .

```

Require: Triangulation (or quadrangulation)  $\mathcal{T}$  of the surface  $M$ , per-element values  $\mu_F$ 
Initialize  $|\mu|_{avg} = 0$ 
for element  $1 \leq F \leq N_{el}$  do
    Update  $|\mu|_{avg} += \frac{|\mu_F|}{N_{el}}$ 
    Normalize  $\mu_F = \frac{\mu_F}{|\mu_F|}$ 
end for
for edge  $1 \leq \alpha \leq N_{edges}$  do
    Initialize  $\mu_\alpha = 0$  and  $l_\alpha = 0$ 
end for
for element  $1 \leq F \leq N_{el}$  do
    for edge  $1 \leq i \leq n_F$  do
        Compute  $\theta_i = \angle(e_1, e_i)$ 
        Update  $\mu_{\alpha_{F,i}} += P(\theta_i)\mu_F$  and  $l_{\alpha_{F,i}} += 1$ , for appropriate local-to-global edge mapping  $\alpha_{F,i}$ 
    end for
end for
for edge  $1 \leq \alpha \leq N_{edges}$  do
    Average  $\mu_\alpha = \frac{\mu_\alpha}{l_\alpha}$ 
end for
for element  $1 \leq F \leq N_{el}$  do
    Initialize  $\mu_F = 0$ 
    for edge  $1 \leq i \leq n_F$  do
        Compute  $\theta_i = \angle(e_1, e_i)$ 
        Update  $\mu_F += \frac{1}{n_F} P^T(\theta_i)\mu_{\alpha_{F,i}}$ , for appropriate local-to-global edge mapping  $\alpha_{F,i}$ 
    end for
end for
for element  $1 \leq F \leq N_{el}$  do
     $\arg \xi_F = \text{atan2}(\mu_F^2, \mu_F^1)$ 
     $\xi_F = |\mu|_{avg} e^{J \arg \xi_F}$ 
end for
return  $\xi_F$ 

```

outstanding question is whether or not an optimal Teichmüller mapping into \mathbb{R}^3 actually exists for a given surface and homotopy class of its boundary data. A more algorithmic concern is how to improve the efficiency of the QC iteration. Although the post-processing Step

3 is an effective way to move a given BC closer to Teichmüller form, it creates the need for an iterative procedure which is relatively slow to converge, especially as a minimizer is approached. If possible, it would be ideal to have a direct way to compute the optimal BC given only the initial surface and boundary data. Finally, it should be mentioned that the QC iteration (as well as every treatment of computational quasiconformal mapping to date) relies on solving a discretized problem which agrees with the smooth theory only in the limit of mesh refinement. It would be highly interesting to see progress toward a fully discrete theory for quasiconformality similar to what is currently being developed for conformality.

ACKNOWLEDGMENTS

The original meshes in Figures 1, 5, 9, and 8 are provided courtesy of the AIM@SHAPE repository. The texture in Figures 2 and 6 is courtesy of “Amonrat rungreangfangsai” and Vecteezy.com. The research of the second author was partially supported by the NSF grant DMS-1912902.

REFERENCES

- E Aulisa, S Bua, and G Boria. 2014. FEMuS Finite Element Multiphysics Solver. *Github repository* (2014).
- Alexander I Bobenko, Ulrich Pinkall, and Boris A Springborn. 2015. Discrete conformal maps and ideal hyperbolic polyhedra. *Geometry & Topology* 19, 4 (2015), 2155–2215.
- Francis E Burstall, Dirk Ferus, Katrin Leschke, Franz Pedit, and Ulrich Pinkall. 2004. *Conformal geometry of surfaces in S^4 and quaternions*. Springer.
- Georgios Daskalopoulos and Richard A Wentworth. 2007. Harmonic maps and Teichmüller theory. *Handbook of Teichmüller theory* 1 (2007), 33–109.
- Gerhard Dziuk and Charles M Elliott. 2013. Finite element methods for surface PDEs. *Acta Numerica* 22 (2013), 289.
- James Eells and Joseph H Sampson. 1964. Harmonic mappings of Riemannian manifolds. *American journal of mathematics* 86, 1 (1964), 109–160.
- Frederick P Gardiner and Nikola Lakic. 2000. Quasiconformal Teichmüller Theory. (2000).
- Anthony Gruber and Eugenio Aulisa. 2020. Computational P-Willmore Flow with Conformal Penalty. *ACM Trans. Graph.* 39, 5, Article 161 (Aug. 2020), 16 pages. <https://doi.org/10.1145/3369387>
- Xianfeng Gu, Yalin Wang, Tony F Chan, Paul M Thompson, and Shing-Tung Yau. 2004. Genus zero surface conformal mapping and its application to brain surface mapping. *IEEE transactions on medical imaging* 23, 8 (2004), 949–958.
- Kin Tat Ho and Lok Ming Lui. 2016. QCMC: quasi-conformal parameterizations for multiply-connected domains. *Advances in Computational Mathematics* 42, 2 (2016), 279–312.
- JH Hubbard. 2006. Teichmüller Theory and Applications to Geometry, Topology and Dynamics, Volume I: Teichmüller Theory. (2006).
- George Kamberov, Franz Pedit, and Peter Norman. 2002. *Quaternions, spinors, and surfaces*. American Mathematical Society.
- Liliya Kharevych, Boris Springborn, and Peter Schröder. 2006. Discrete Conformal Mappings via Circle Patterns. *ACM Trans. Graph.* 25, 2 (April 2006), 412–438. <https://doi.org/10.1145/1138450.1138461>
- Yin Tat Lee, Ka Chun Lam, and Lok Ming Lui. 2016. Landmark-matching transformation with large deformation via n-dimensional quasi-conformal maps. *Journal of Scientific Computing* 67, 3 (2016), 926–954.
- B. Lévy, S. Petitjean, N. Ray, and J. Maillot. 2002. Least squares conformal maps for automatic texture atlas generation. In *ACM transactions on graphics (TOG)*, Vol. 21. ACM, 362–371.
- Yaron Lipman. 2012. Bounded Distortion Mapping Spaces for Triangular Meshes. *ACM Trans. Graph.* 31, 4, Article 108 (July 2012), 13 pages.
- Lok Ming Lui, Xianfeng Gu, and Shing-Tung Yau. 2015. Convergence of an iterative algorithm for Teichmüller maps via harmonic energy optimization. *Math. Comp.* 84, 296 (2015), 2823–2842.
- Lok Ming Lui, Ka Chun Lam, Shing-Tung Yau, and Xianfeng Gu. 2014. Teichmuller mapping (t-map) and its applications to landmark matching registration. *SIAM Journal on Imaging Sciences* 7, 1 (2014), 391–426.
- Ting Wei Meng, Gary Pui-Tung Choi, and Lok Ming Lui. 2016. TEMPO: Feature-Endowed Teichmüller Extremal Mappings of Point Clouds. *SIAM Journal on Imaging Sciences* 9, 4 (2016), 1922–1962. <https://doi.org/10.1137/15m1049117>
- Xianshu Nian and Falai Chen. 2016. Planar domain parameterization for isogeometric analysis based on Teichmüller mapping. *Computer Methods in Applied Mechanics and Engineering* 311 (2016), 41–55.
- Jing Peng, Douglas R Heisterkamp, and Ho Kwok Dai. 2004. Adaptive quasiconformal kernel nearest neighbor classification. *IEEE Transactions on Pattern Analysis and Machine Intelligence* 26, 5 (2004), 656–661.
- Ulrich Pinkall and Konrad Polthier. 1993. Computing discrete minimal surfaces and their conjugates. *Experimental mathematics* 2, 1 (1993), 15–36.
- Di Qiu, Ka-Chun Lam, and Lok-Ming Lui. 2019. Computing Quasi-Conformal Folds. *SIAM Journal on Imaging Sciences* 12, 3 (2019), 1392–1424.
- Edgar Reich. 2002.. Extremal Quasi-conformal Mappings of the Disk. *Handbook of Complex Analysis: Geometric Function Theory* 1, Chapter 3 (2002), 75–135.
- Rohan Sawhney and Keenan Crane. 2017. Boundary First Flattening. *ACM Trans. Graph.* 37, 1, Article 5 (Dec. 2017), 14 pages. <https://doi.org/10.1145/3132705>
- Boris Schäling. 2011. *The boost C++ libraries*. Boris Schäling.
- Boris Springborn, Peter Schröder, and Ulrich Pinkall. 2008. Conformal Equivalence of Triangular Meshes. *ACM Trans. Graph.* 27, 3 (Aug. 2008), 1–11. <https://doi.org/10.1145/1360612.1360676>
- Kurt Strebel. 1978. On quasiconformal mappings of open Riemann surfaces. *Commentarii Mathematici Helvetici* 53, 1 (1978), 301–321.
- Kurt Strebel. 1984. Quadratic differentials. In *Quadratic Differentials*. Springer, 16–26.
- Lloyd N Trefethen. 2020. Numerical conformal mapping with rational functions. *Computational Methods and Function Theory* 20, 3 (2020), 369–387.
- Ofir Weber, Ashish Myles, and Denis Zorin. 2012. Computing extremal quasiconformal maps. In *Computer Graphics Forum*, Vol. 31. Wiley Online Library, 1679–1689.
- Jinlan Xu, Hongmei Kang, and Falai Chen. 2018. Content-aware image resizing using quasi-conformal mapping. *The Visual Computer* 34, 3 (2018), 431–442.
- Yi-Jun Yang and Wei Zeng. 2020. Quasiconformal rectilinear map. *Graphical Models* 107 (January 2020), 101057. <https://doi.org/10.1016/j.gmod.2019.101057>
- Wei Zeng and Xianfeng David Gu. 2011. Registration for 3D surfaces with large deformations using quasi-conformal curvature flow. In *CVPR 2011*. IEEE, 2457–2464.
- Wei Zeng, Lok Ming Lui, Feng Luo, Tony Fan-Cheong Chan, Shing-Tung Yau, and David Xianfeng Gu. 2012. Computing quasiconformal maps using an auxiliary metric and discrete curvature flow. *Numer. Math.* 121, 4 (2012), 671–703.

A APPENDIX: EQUIVALENCE

To establish the equivalence of Definition 2.7 and Definition 2.8, suppose Definition 2.7 holds. Then, $\mu : TM \rightarrow TM$ is a \mathbb{C} -antilinear mapping satisfying $|\mu|_\infty < 1$ and $df^- = df^+ \circ \mu$. But, this means that given any local basis section $v \subset TM$, we have

$$\mu(v) = \mu^1(v)v + \mu^2(v)Jv,$$

for some functions $\mu^i : TM \rightarrow \mathbb{R}$. Consequently, it follows that

$$\begin{aligned} df^+ \circ \mu(v) &= df^+ \left(\mu^1(v)v + \mu^2(v)Jv \right) \\ &= \mu^1(v)df^+(v) + \mu^2(v)*df^+(v) \\ &= \left(\mu^1(v) + \mu^2(v)N \right) df^+(v) = \tilde{\mu}(v)df^+(v), \end{aligned}$$

where $\tilde{\mu} = \mu^1 + J\mu^2$ is a \mathbb{C} -valued function on TM which transforms as in Lemma 2.9. Therefore, $\tilde{\mu}$ satisfies Definition 2.8. Conversely, it is readily verified (by repeating this argument backwards) that any appropriate function $\tilde{\mu} : TM \rightarrow \mathbb{C}$ yields a $\mu : TM \rightarrow TM$ as seen in Definition 2.7.